Design of a Multifingered Robot Hand and User Interface for Force-Transparent Teleoperation

Luke Batteas, Oliver Sterling-Angus, Yufeng Yang, Patrick Dills, Kevin Lynch, and Ed Colgate
Center for Robotics and Biosystems, Northwestern University

***Abstract*— Teleoperators consisting of leaders (e.g. haptic interfaces) and followers (e.g., robot manipulators) have the potential to enable remote completion of many useful tasks; however, for tasks that require high manual dexterity, the limitations of these systems becomes more apparent and problematic. One notable discrepancy between teleoperation and direct human manipulation is the wealth of tactile and kinesthetic information intrinsically available to humans. Current robotic manipulators, especially hands, are not well equipped to measure and control tactile and kinesthetic data. Moreover, current haptic displays, when used as leaders, are not well-equipped to display those data while remaining in tight coordination with followers. In this work, we explore a co-design philosophy to enable highly transparent fingertip-level force feedback for teleoperation of multifingered hands.**

I. Introduction

Teleoperation enables human operators, controlling robotic avatars, to remotely perform useful tasks that are too nascent, varied, or high-consequence to be automated. Under a typical bilateral teleoperation scheme, the robotic avatar records and transmits visual, audio, force, and tactile data to the human operator, who interprets and acts on this data. While audio and visual information can be faithfully displayed with a virtual reality (VR) headset, haptic displays struggle to do the same for force and tactile data. For tasks involving manipulation, this often leads to operators relying on visual feedback as a supplement for sub-par or nonexistent haptic feedback [1], [2]. In turn, teleoperated dexterous tasks that demand this haptic feedback must typically be completed at a much slower rate, if at all [3].

In particular, force feedback provides essential information relating to the strength of a grasp, as well as providing key information about the manipulability of a grasped object. Most existing teleoperation systems can provide only a few degrees of force feedback— no more than one per finger [1], [2], [3], [4]. The limited nature of this feedback means that the force information provided to an operator is at best incomplete as reaction forces orthogonal to the kinesthetic display direction cannot be presented. Similarly, many wearable finger haptic displays have equally low-dimensional outputs [5], [6], [7], [8]. While grounded displays are quite capable of providing multi-directional force feedback, in-hand manipulation tasks often cause fingers to obstruct or collide with the links of the device [9], [10]. In contrast to this, Ferguson et al. have developed a 3-DoF-per-finger kinesthetic display aimed at rehabilitation [11]. Higher DoF displays would enable full force reconstruction at the fingertips, providing more accurate feedback. However, even with a high DoF haptic device, estimating and displaying environmental forces affecting a robotic hand is non-trivial.

Our hypothesis is that the co-design of a robot hand in conjunction with a kinesthetic haptic device specifically for teleoperation will result in a system that, under bilateral control, will be capable of faithfully displaying environmental forces to a human operator. In this work we discuss the design of a 9 DoF—3 DoF per finger—haptic interface and paired robotic manipulator shown in Figure 1.

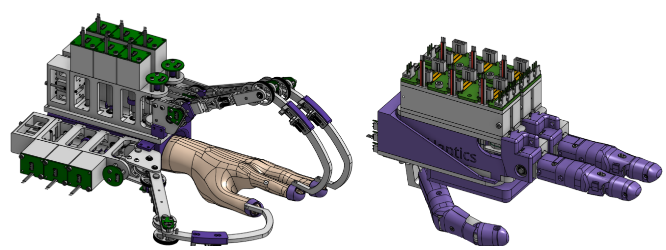

Fig. 1. 9 DoF, 3 fingered, robotic hand and co-designed haptic interface

II. Design and Control

A. Design philosophy

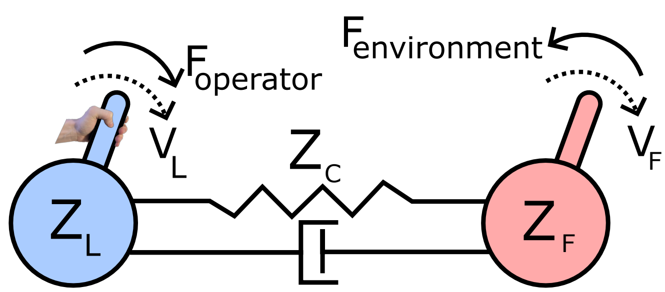

Fig. 2. A one-degree-of-freedom teleoperation device which transmits operator force to the environment and environmental forces to the operator.

Let us briefly consider a one-degree-of-freedom bilateral system shown in Figure 2. The two sides, the leader and the follower, are coupled via a virtual impedance provided by the controller. We can model this system as a series of impedances where impedance is given by

$$Z(s) = \frac{F(s)}{V(s)}. \quad (1)$$

The mechanical impedances of the leader and follower devices are given by Z_L and Z_F, respectively, and the virtual impedance of the controller is given by Z_C. As the operator commands the velocity of the leader device V_L and experiences the force feedback of $F_{operator}$, the follower device is compelled to move due to the coupling and is also subject to $F_{environment}$,

$$\begin{bmatrix} F_{operator} \\ -F_{environment} \end{bmatrix} = \begin{bmatrix} Z_L + Z_C & -Z_C \\ -Z_C & Z_F + Z_C \end{bmatrix} \begin{bmatrix} V_L \\ V_F \end{bmatrix}. \quad (2)$$

We shall explore the case in which the environmental force is supplied by an environmental impedance Z_E. In the ideal case, our devices and control would enable the operator to experience the impedance of the environment, Z_E. Equation (2) can be simplified to

$$\begin{bmatrix} F_{operator} \\ -Z_E V_F \end{bmatrix} = \begin{bmatrix} Z_L + Z_C & -Z_C \\ -Z_C & Z_F + Z_C \end{bmatrix} \begin{bmatrix} V_L \\ V_F \end{bmatrix}. \quad (3)$$

Examining the bottom row of the matrix, we can solve for V_L as a function of V_F

$$\frac{Z_c}{Z_F + Z_C + Z_E} V_L = V_F. \quad (4)$$

Substituting Equation (4) into Equation (3) and combining terms yields the effective impedance of the leader device

$$\frac{F_{operator}}{V_L} = \frac{Z_L Z_F + (Z_L + Z_F) Z_C + Z_E (Z_L + Z_C)}{Z_F + Z_C + Z_E}. \quad (5)$$

While we are interested in conveying a whole range of Z_E, we will examine two boundary cases to gain insight as to how we should design our system impedances.

In the case where the magnitude of Z_E is near 0 (i.e., no contact is occurring), the effective impedance is a function of the system impedances. As we are trying to match Z_E, we must minimize the magnitude of Z_L and Z_F. If we do not minimize Z_F in addition to Z_L then we have arrived at the current teleoperation paradigm, wherein highly transparent haptic interfaces have been connected to robotic manipulators which have not been designed for teleoperation.

In the case where the magnitude of Z_E is large (e.g., when contacting a rigid object), we may suspect that since the impedance is being conveyed through Z_C, Z_C must be larger than Z_E.

Under these conditions where by magnitude, $Z_C >> Z_E >> Z_L, Z_F$ (in the interest of brevity we assume this relationship to hold until some relevant bandwidth ω_c) we can see that the effective impedance reduces to

$$\frac{F_{operator}}{V_L} = Z_E.$$

Although this is only a one-degree-of-freedom example, the ideas explored within it guide our design process. Critically, the design of both the leader and follower devices affects the performance of the system. This leads to our co-design philosophy, where rather than purchase a commercial robotic manipulator, we seek to design one in parallel to a haptic interface to ensure the quality of the bilateral connection. Put simply, we seek to minimize the mechanical impedance of both the leader and follower devices and maximize the impedance of the controlled virtual coupling. In following this philosophy, we have some confidence that this teleoperation system will be capable of faithfully displaying a wide range of impedances encountered by the follower device. In addition to the design objectives discussed above, the overall mass of the system is also a consideration, as both devices are intended to mount to robot arms in future work, to move the follower hand and to provide grounded force feedback to the leader.

B. Device design

We will extend the leader-follower example above specifically to finger dexterity, where the leader device is a haptic interface that accepts operator commands and provides feedback, and the follower device is a robotic manipulator. In pursuit of our design objectives, we must make some sacrifices. Rather than developing a teleoperator device supplying all fingers with force feedback, we will concentrate mass where it benefits dexterity the most, the middle finger, index finger, and thumb. These three fingers are responsible for most dexterous tasks whereas the remaining digits are mostly used to supply higher forces to better fixture larger objects. Overall, the teleoperation system is 9 DoF, offering 3 DoF of force feedback per finger, sufficient to reconstruct three-axis reaction forces. This enables the freedom to form common dexterous grasps such as pinch and key grasps allowing for interesting and challenging tasks such as unscrewing lids, manipulating tools such as soldering irons, and in-hand manipulation of small objects.

Due to kinematic similarities, the device is modularized, such that each finger is identical aside from variations in link lengths for the thumb module. Below, we will explore the design of one of these modules for each device.

1) Robotic finger: For the robotic finger (Figure 3A), the three actuated degrees of freedom are similar to those present in a human finger: one degree of freedom for abduction-adduction at the Metacarpophalangeal joint (MCP) and two degrees of freedom for flexion-extension (MCP and Proximal Interphalangeal (PIP) joints). The flexion of the Distal Interphalangeal joint (DIP) is coupled to flexion of the PIP joint by a four-bar mechanism to improve grips of objects and to achieve approximately anthropomorphic motion. We constrained the outer profile of the finger to the size and shape of a human finger. As the device is intended to be used by a human operator on human-scaled objects, the anthropomorphic constraint is hypothesized to allow more predictable motion from the operators' input as well as having the proper scale for interactions with objects. In addition to the outer profile of the finger, the actuator package was designed to be as small as possible, having a width of 26.35 mm, which enables placing several fingers in close proximity. In total, the mass of a single finger, including its actuator package, is 400 g. In addition to the anthropomorphism of the device, we spent significant effort on minimizing the mechanical impedance of the device through the both the minimization of inertias and the design and selection of actuators and tendons, which is discussed below.

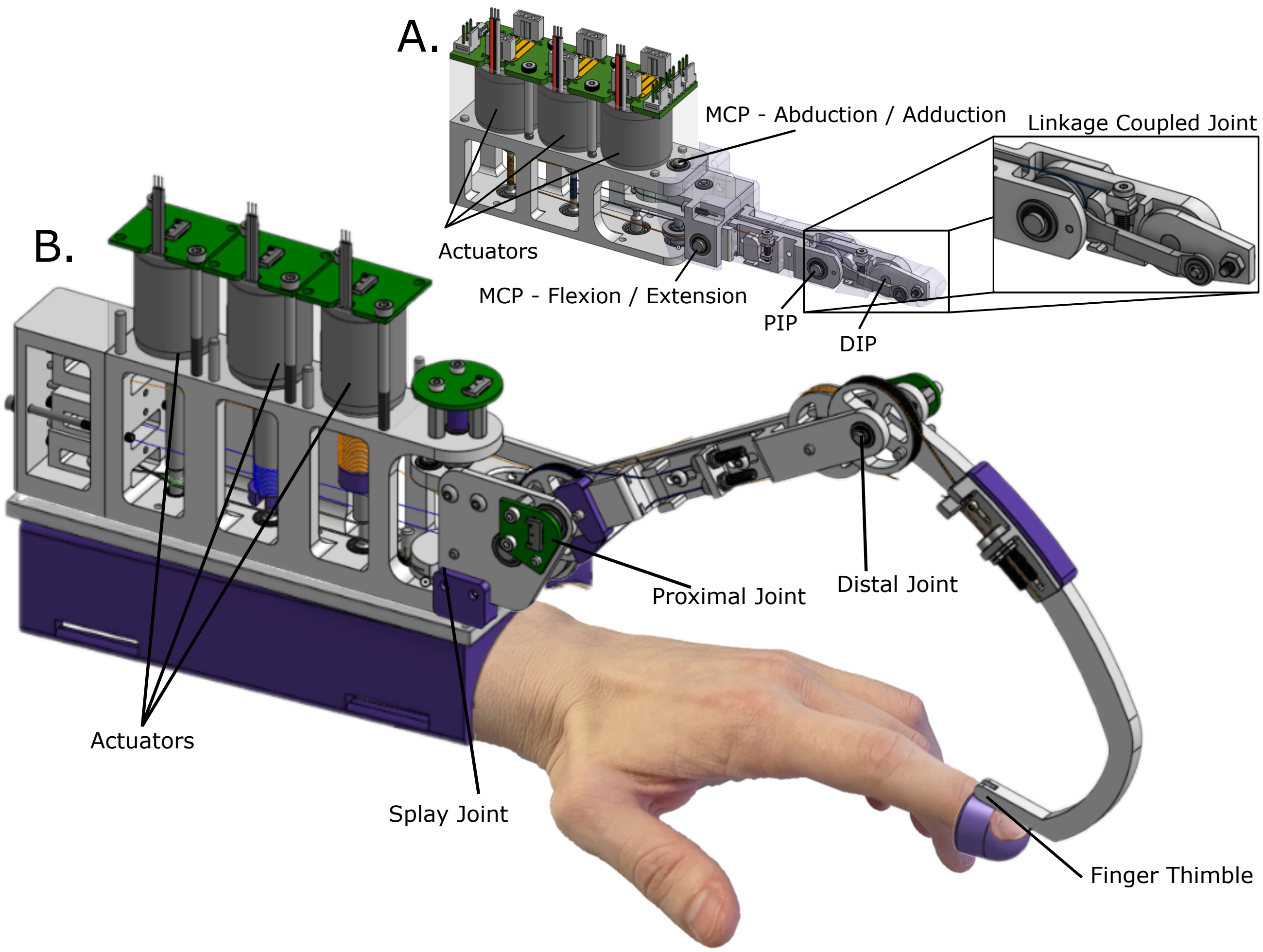

Fig. 3. A. The 3-DoF robotic finger which is anthropomorphic in both size and kinematics, B. The 3-DoF haptic exo-finger attached to a finger

2) Haptic interface: For the haptic interface (Figure 3B), the three degrees of freedom are kinematically similar to the robotic finger, offering one splaying joint and two in the flexion-extension plane.

The geometry of the links were specifically designed to avoid contact with the human finger, allowing the links to wrap around finger over its full range of motion, avoiding contact until the full closure of the fist.

The decision was made to mount the haptic interface to the forearm, proximal to the wrist, to minimize the mass placed on the back of the hand. This necessarily couples the motion of the wrist, to the motions of the linkages. In this work, the wrist is fixed so this coupling is unimportant. Future work will include an extension of the device which will sensorize the wrist to uncouple the motion. The mass of one exo-finger system is 850 g although the linkage itself weights only 200 g.

One significant challenge in the design of the haptic interface is the attachment to the operator's fingers as well as general affordance for the operator. Since there can be significant variation in a human's finger lengths and shape, designing an attachment to fit many different humans was quite difficult. Compliant elements like elastic bands drastically drop the mechanical stiffness of the device, preventing higher stiffnesses from being rendered. After significant iteration, we designed and FDM printed PLA finger thimbles to provide a comfortable and secure attachment to the finger while retaining a high stiffness. Several different sizes of thimbles were fabricated and can be quickly swapped out at the end of the links. One very critical element of the finger thimble is the ball and socket joint that connects it to the links of the exo-finger. Due to slight kinematic differences between people, it is not possible to match the kinematics of each potential operator. With the freedom afforded by the ball-and-socket joint, we can focus on obtaining the correct positioning, letting orientation remain whatever is natural to the operator. As with the robotic finger, the mechanical impedance is minimized through minimizing inertia and friction in addition to intelligent selection of actuators and tendons.

C. Actuators

The actuators in the system have several competing design objectives. We sought to minimize both the mass and the rotor inertia while maximizing the continuous torque. The rotor inertia contributes to the mechanical impedance of the system while the torque limits the maximum displayable force. A tendon transmission (discussed below) was implemented to increase the torque. However, this increases the contribution of the rotor inertia to the mechanical impedance. Additionally, we would like smooth torque generation free of cogging, since this can distort the coupling between the leader and follower. For these reasons, we selected brushless DC (BLDC) motors which provide high torque density and smooth torque profiles. Furthermore, we selected frameless motors to tightly integrate the actuators into the design, minimizing unnecessary mass. In practice, we find that selecting the largest motor subject to one's size constraints results in the optimal torque while minimizing the reflected rotor inertia due to the transmission. We selected two different models of BLDC motors from Mosrac Motors, due to different size constraints for each device. The U2523 is a 31.5 W motor one capable of producing 75 mNm and the U2535 is a 37.3 W 120 mNm for the devices. All motors are controlled using field-oriented control to ensure smooth torque production at all speeds. An anti-cogging map is not currently implemented, but will be considered in the future.

D. Tendons

The tendons play a signification role in the design, offering a backlash-free transmission between the motors and the joints. Additionally, in comparison to other transmissions, they are very light and compact. While it is possible to achieve only moderate (∼10:1) transmission ratios within the given size constraints, this is sufficient for our use case and limits the increase in perceived inertia.

The tendon material is important because the stiffness of the tendon limits the maximum impedance of the virtual coupling. Additionally, the maximum load of the tendons imposes a limitation on the maximum force the device can exert. The tendon material used in the design is a braided polymer fishing line of 0.36 mm diameter. The polymer fishing line was measured to have a Young's Modulus of about 14 GPa corresponding to a stiffness of 14 N/mm with a tendon length of 100 mm.

Both devices use a single tendon per joint (thus, 'N' rather than 'N+1' or '2N' architectures). This was done to minimize motor mass, but required us to incorporate tendon tensioning components. In the haptic interface, distal transmissions were incorporated to maximize the mechanical stiffness as well as minimize the tendon tension [12]. Unlike some other designs [11], [13], Bowden cables were not used to aid in routing. The friction and hysteresis introduced by a Bowden cable increase the mechanical impedance of the device and obfuscate the actual torque applied to the joints by the actuators. In our design, the tendons route though a series of pulleys supported by ball bearings.

E. Control

We have implemented the bilateral control scheme shown in Figure 4. The end effectors of the two devices are coupled via a virtual spring and damper. As a result, misalignment between the leader and follower end effector positions/velocities generates a restoring force. If the robot finger encounters an obstacle, forces develop in the virtual spring/damper, and these forces are transmitted to the human fingertip as kinesthetic feedback.

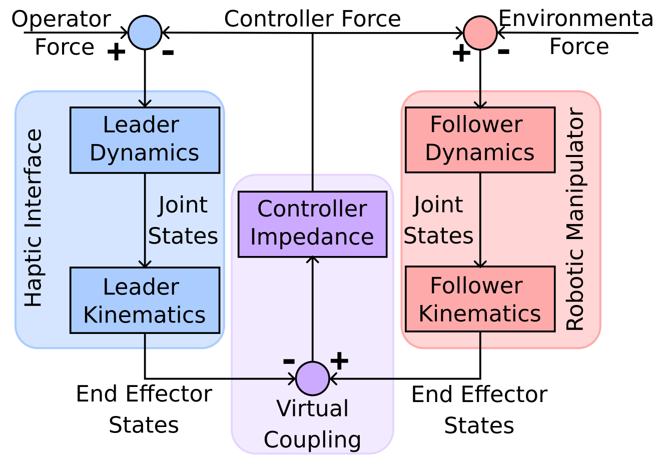

Fig. 4. Bilateral control scheme coupling the leader and follower device

III. Future Work

At this time, one robot finger and one haptic finger have been manufactured and assembled as shown in Figure 5. The immediate next steps will be the characterization of the mechanical impedances along with coupled dexterous task experimentation at different virtual impedance levels.

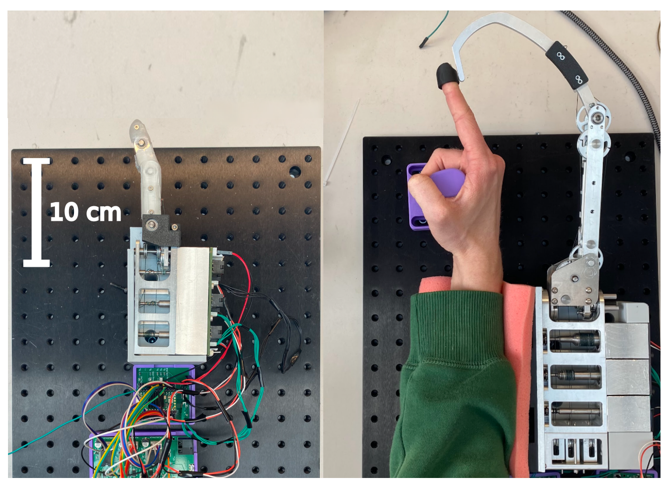

Fig. 5. Assembled testbeds of one finger and one exo-finger device

Acknowledgment

This research was partially supported by two DOE Office of Science program offices: Advanced Scientific Computing Research (ASCR) and Isotope R&D and Production (IRP). The authors would like to acknowledge the contributions of Northwestern's Robot Design Student Studio Class of 2024, particularly Chris Jung and Yanni Kechriotis, for their work on a first iteration of the design.

REFERENCES

[1] J. A. Fishel et al., “Tactile Telerobots for Dull, Dirty, Dangerous, and Inaccessible Tasks,” in 2020 IEEE International Conference on Robotics and Automation (ICRA), May 2020, pp. 11305–11310. doi: 10.1109/ICRA40945.2020.9196888.

[2] T. Z. Zhao, V. Kumar, S. Levine, and C. Finn, “Learning Fine-Grained Bimanual Manipulation with Low-Cost Hardware,” Apr. 23, 2023, arXiv: arXiv:2304.13705. doi: 10.48550/arXiv.2304.13705.

[3] T. Buckley and J. E. Colgate, ”Dexterous Manipulation with a Bi-Manual Anthropomorphic Teleoperation Robot,” in Proc. 3rd Workshop Toward Robot Avatars, IEEE/RSJ International Conference on Intelligent Robots and Systems (IROS), Abu Dhabi, UAE, Oct. 2024,

[4] M. Schwarz, C. Lenz, A. Rochow, M. Schreiber, and S. Behnke, “NimbRo Avatar: Interactive Immersive Telepresence with Force-Feedback Telemanipulation,” Sep. 28, 2021, arXiv: arXiv:2109.13772. doi: 10.48550/arXiv.2109.13772.

[5] D. Wang, M. Song, A. Naqash, Y. Zheng, W. Xu, and Y. Zhang, “Toward Whole-Hand Kinesthetic Feedback: A Survey of Force Feedback Gloves,” IEEE Trans. Haptics, vol. 12, no. 2, pp. 189–204, Apr. 2019, doi: 10.1109/TOH.2018.2879812.

[6] F. Gosselin, C. Andriot, F. Keith, F. Louveau, G. Briantais, and P. Chambaud, “Design and Integration of a Dexterous Interface with Hybrid Haptic Feedback:,” in Proceedings of the 17th International Conference on Informatics in Control, Automation and Robotics, Lieusaint - Paris, France: SCITEPRESS - Science and Technology Publications, 2020, pp. 455–463. doi: 10.5220/0009831204550463.

[7] D. Leonardis et al., “Hand Teleoperation with Combined Kinaesthetic and Tactile Feedback: A Full Upper Limb Exoskeleton Interface Enhanced by Tactile Linear Actuators,” Robotics, vol. 13, no. 8, Art. no. 8, Aug. 2024, doi: 10.3390/robotics13080119.

[8] H. Zhang, S. Hu, Z. Yuan, and H. Xu, “DOGlove: Dexterous Manipulation with a Low-Cost Open-Source Haptic Force Feedback Glove,” Feb. 11, 2025, arXiv: arXiv:2502.07730. doi: 10.48550/arXiv.2502.07730.

[9] T. Endo et al., “Five-fingered haptic interface robot: HIRO III,” in World Haptics 2009 - Third Joint EuroHaptics conference and Symposium on Haptic Interfaces for Virtual Environment and Teleoperator Systems, Mar. 2009, pp. 458–463. doi: 10.1109/WHC.2009.4810812.

[10] L. Liu, S. Miyake, K. Akahane, and M. Sato, “Development of string-based multi-finger haptic interface SPIDAR-MF,” in 2013 23rd International Conference on Artificial Reality and Telexistence (ICAT), Dec. 2013, pp. 67–71. doi: 10.1109/ICAT.2013.6728908.

[11] P. W. Ferguson, J. Sun, J. Ma, J. Perry, and J. Rosen, “On the OTHER Hand: A Bilateral, Reconfigurable Hand Exoskeleton With Opposable Thumbs for Use With Upper Limb Exoskeletons,” IEEE Trans. Med. Robot. Bionics, vol. 6, no. 3, pp. 1158–1169, Aug. 2024, doi: 10.1109/TMRB.2024.3421513.

[12] W. T. Townsend and J. K. Salisbury, “Mechanical Design for Whole-Arm Manipulation,” in Robots and Biological Systems: Towards a New Bionics?, P. Dario, G. Sandini, and P. Aebischer, Eds., Berlin, Heidelberg: Springer, 1993, pp. 153–164. doi: 10.1007/978-3-642-58069-7_9.

[13] L. B. Bridgwater et al., “The Robonaut 2 hand - designed to do work with tools,” in 2012 IEEE International Conference on Robotics and Automation, St Paul, MN, USA: IEEE, May 2012, pp. 3425–3430. doi: 10.1109/ICRA.2012.6224772.